Hindawi Publishing Corporation
International Journal of Antennas and Propagation
Volume 2014, Article ID 975109, 8 pages
http://dx.doi.org/10.1155/2014/975109

Research Article

Capacity of κ-μ Shadowed Fading Channels

Celia García-Corrales, Francisco J. Cañete, and José F. Paris

Departamento Ingeniería de Comunicaciones, ETS Ingeniería de Telecomunicacion, Universidad de Malaga, E-29071 Málaga, Spain

Correspondence should be addressed to Celia García-Corrales; celia@ic.uma.es

Received 9 May 2014; Accepted 10 July 2014; Published 24 July 2014

Academic Editor: Theodoros Tsiftsis

The ergodic capacity of fading channels modeled with a κ-μ shadowed distribution is investigated to derive closed-form expressions. The κ-μ shadowed distribution is of particular interest because it contains, as special cases, other classical ones like one-side Gaussian, Rayleigh, Rician, Nakagami-m, κ-μ, and Rician shadowed distributions. The paper discusses the physical meaning of the distribution parameter variations and also their impact on the channel capacity. These results can be used to study the behavior of different channels like the ones in underwater acoustic communications, land mobile satellite systems, body centric communications, and other wireless communication applications. The analytical closed-form expression results are validated with numerical simulations.

1. Introduction

The propagation of radio waves or acoustic waves, used as data carriers, in realistic scenarios where either the transmitter, receiver, or surrounding objects are moving is quite complex. The amplitude and phase instantaneous values of the incident waves exhibit rapid variations according to the interaction patterns with the environment. This interaction produces phenomena like reflection, diffraction, and scattering of the waves on the object surfaces [1]. All this makes the problem of modeling the communication channel behavior almost unmanageable with a deterministic approach. An alternative strategy is to formulate mathematical models that reach a reasonable similarity to the expected signal at the receiver from a statistical approach. Such models try to reproduce the received signal according to different time scales. On the one hand, at a large time scale, there is a path loss modeling that estimates the mean signal strength, which is notably influenced by the transmission distance. On the other hand, there is a fading modeling, at a shorter scale, to represent the rapid fluctuations around the mean due essentially to multipath propagation. Even for this fading, two levels of approximation are usual: a long-term fading due to the influence of macroscopic movements in the environment (associated with a channel time-varying behavior) that is slower than a short-term fading, which is caused by variations in the superposition of the different wave components associated with the transmitted signal, even in a quasistatic environment [2, 3]. There exist many statistical fading models and the κ-μ distribution has been used in some of them to represent the received signal level in a flexible way [4–10].

The present work focused on the short-term, narrowband, fading experienced in multipath propagation scenarios with a line-of-sight condition. Besides the multipath fading, shadowing of the dominant components is also investigated. There are two kinds of models that consider shadowing: in the first one, shadowing is assumed to change the whole signal power (composed of the dominant components and the scattered waves) [11–14]. In the second type of models, the shadowing is considered to affect only the power of the dominant components, like the Rician shadowed model [15]. This latter model was initially employed to fit experimental data from land mobile satellite channels and lately has also been applied to actual underwater acoustic communications (UAC) channels [16].

The present work is based on the *κ-μ shadowed distribution model*, first proposed in [17], which belongs to the second

type of shadowing models and achieves a better fit to UAC channels measurements.

The paper is organized as follows: first, the system model is addressed in Section 2, explaining its physical interpretation and providing some fundamental statistics. In Section 3, the mathematical analysis of the ergodic capacity of the channel for the assumed model is presented, whereas, in Section 4, numerical simulations that support the analytical results are discussed. Finally, some conclusions are given in the last section.

2. System Model

The purpose of this section is to define the framework of the problem and to help the reader to follow the remainder of the paper. To this end, a brief summary of the physical model underneath the κ-μ shadowed distribution is given and the main statistical functions of this distribution are reviewed.

2.1. Physical Model. In the physical model for the κ-μ shadowed distribution [17], the received power W can be expressed in terms of the in-phase and quadrature components of the fading signal by

$$W = \sum_{i=1}^{n} \left(X_i + \xi p_i\right)^2 + \left(Y_i + \xi q_i\right)^2, \tag{1}$$

where n is a natural number, X_i and Y_i are mutually independent Gaussian processes (with $E[X_i] = E[Y_i] = 0$, $E[X_i^2] = E[Y_i^2] = \sigma^2$), and p_i and q_i are real numbers. Each term of the sum represents a multipath cluster and hence n is the number of clusters. The random variable $X_i + jY_i$ models the scattered components of the ith cluster, which is a circularly symmetric complex Gaussian since the number of components is considered large enough so that the central-limit theorem applies. In each cluster, the total power of the scattered components is $2\sigma^2$, while the dominant component of the ith cluster is given by the complex random variable $\xi p_i + j\xi q_i$, whose power is $p_i^2 + q_i^2$ as ξ is a power-normalized random variable.

The following are the main parameters to formulate the κ-μ shadowed distribution.

(i) m–parameter: all the dominant components exhibit a common shadowing fluctuation that is represented by the random amplitude ξ, that is, a Nakagami-m random variable with shaping parameter m and $E[\xi^2] = 1$.

(ii) μ-parameter: the natural number of clusters n can be replaced in (1) by the nonnegative real extension μ, which leads to a more general and flexible distribution.

(iii) κ-parameter: the ratio between the power of the dominant components and the power of the scattered waves is represented by κ that is defined as $\kappa = (\sum_{i=1}^{\mu} p_i^2 + q_i^2)/(2\sigma^2\mu)$, when μ is a natural number.

Assume $\gamma \sim \mathcal{S}_{\kappa\mu}(\overline{\gamma}; \kappa, \mu, m)$ is a κ-μ shadowed random variable with mean $\overline{\gamma}$ and real nonnegative shaping parameters κ, μ, and m. γ represents the instantaneous signal to noise ratio at the receiver and models the fading channel. It can be defined as $\gamma \triangleq \overline{\gamma} W/\overline{W}$, where $\overline{\gamma} \triangleq E[\gamma]$ and $\overline{W} = E[W] = 2\sigma^2\mu + \sum_{i=1}^{\mu} p_i^2 + q_i^2$ (for a natural μ).

2.2. Fundamental Statistics. In this part, the most important statistical functions corresponding to the κ-μ shadowed distribution are presented (see details in [17]).

The probability density function (PDF) of γ is given by

$$f_\gamma(\gamma) = \frac{\mu^\mu m^m (1+\kappa)^\mu}{\Gamma(\mu)\,\overline{\gamma}(\mu\kappa + m)^m} \left(\frac{\gamma}{\overline{\gamma}}\right)^{\mu-1} \times e^{-\mu(1+\kappa)\gamma/\overline{\gamma}}\, {}_1F_1\left(m, \mu; \frac{\mu^2\kappa(1+\kappa)}{\mu\kappa + m}\frac{\gamma}{\overline{\gamma}}\right), \tag{2}$$

where ${}_1F_1(\cdot)$ is the confluent hypergeometric function defined in [19].

The associated cumulative density function (CDF) of γ is given by

$$F_\gamma(\gamma) = \frac{\mu^{\mu-1} m^m (1+\kappa)^\mu}{\Gamma(\mu)(\mu\kappa + m)^m} \left(\frac{1}{\overline{\gamma}}\right)^\mu \gamma^\mu \times \Phi_2\left(\mu - m, m; \mu + 1; -\frac{\mu(1+\kappa)\gamma}{\overline{\gamma}}, -\frac{\mu(1+\kappa)}{\overline{\gamma}}\frac{m\gamma}{\mu\kappa + m}\right), \tag{3}$$

where $\Phi_2(\cdot)$ is the bivariate confluent hypergeometric function defined in [19].

The moment generating function (MGF) of γ is given by

$$\mathcal{M}_\gamma(s) \triangleq E\left[e^{\gamma s}\right] = \frac{(-\mu)^\mu m^m (1+\kappa)^\mu}{\overline{\gamma}^\mu(\mu\kappa + m)^m} \times \frac{\left(s - (\mu(1+\kappa)/\overline{\gamma})\right)^{m-\mu}}{\left(s - (\mu(1+\kappa)/\overline{\gamma})\left(m/(\mu\kappa + m)\right)\right)^m}. \tag{4}$$

3. Ergodic Capacity Analysis

For the physical model under consideration, the ergodic capacity of the channel (in bit/s/Hz) can be calculated [3] from

$$C = \int_0^\infty \log_2(1+\gamma)\, f_\gamma(\gamma)\, d\gamma, \tag{5}$$

which, after substituting (2), leads to

$$C = \int_0^\infty \log_2(1+\gamma)\, \frac{\mu^\mu m^m (1+\kappa)^\mu}{\Gamma(\mu)\,\overline{\gamma}(\mu\kappa+m)^m}\left(\frac{\gamma}{\overline{\gamma}}\right)^{\mu-1} \times e^{-\mu(1+\kappa)\gamma/\overline{\gamma}}\, {}_1F_1\left(m,\mu;\frac{\mu^2\kappa(1+\kappa)}{\mu\kappa+m}\frac{\gamma}{\overline{\gamma}}\right) d\gamma. \tag{6}$$

In order to find the analytical solution to this equation, the Meijer G-function is going to be introduced. This is a very general function, intended to include many of the known special functions as particular cases, which is represented by a Mellin-Barnes type of contour integral (see 9.3 in [19]). In order to be consistent with (10), the variable of integration in the definition shown in [19] has been changed to $-s$, as follows:

$$G_{p_0,q_0}^{m_0,n_0}\left(\begin{matrix}a_1,a_2,\ldots,a_{n_0},a_{n_0+1},\ldots,a_{p_0}\\ b_1,b_2,\ldots,b_{m_0},b_{m_0+1},\ldots,b_{q_0}\end{matrix}\,\middle|\, z\right) = G_{p_0,q_0}^{m_0,n_0}\left(\begin{matrix}\mathbf{a_{p_0}}\\ \mathbf{b_{q_0}}\end{matrix}\,\middle|\, z\right) = \frac{1}{2\pi i}\int_L \Psi(s)\, z^{-s} ds, \tag{7}$$

where

$$\Psi(s) = \frac{\prod_{j=1}^{m_0}\Gamma(b_j+s)\prod_{k=1}^{n_0}\Gamma(1-a_k-s)}{\prod_{k=n_0+1}^{p_0}\Gamma(a_k+s)\prod_{j=m_0+1}^{q_0}\Gamma(1-b_j-s)}, \tag{8}$$

$0 \le m_0 \le q_0$, $0 \le n_0 \le p_0$, and the poles of $\Gamma(b_j+s)$ must not coincide with the poles of $\Gamma(1-a_k-s)$ (with $j=1,\ldots,m_0$ and $k=1,\ldots,n_0$). L is a suitable closed contour in the complex s-plane which can be chosen among three types of integration paths.

Three special functions can be found in (6): the logarithm, the exponential, and the confluent hypergeometric function. They can be expressed in terms of their Meijer G-identities and then the ergodic capacity can be evaluated using the integration theorem for Meijer G-functions [20] to obtain

$$\int_0^\infty t^{\alpha-1} G_{p_1,q_1}^{m_1,n_1}\left(\begin{matrix}\mathbf{a_{1p_1}}\\ \mathbf{b_{1q_1}}\end{matrix}\,\middle|\, zt\right) G_{p_2,q_2}^{m_2,n_2}\left(\begin{matrix}\mathbf{a_{2p_2}}\\ \mathbf{b_{2q_2}}\end{matrix}\,\middle|\, xt\right) \times G_{p_3,q_3}^{m_3,n_3}\left(\begin{matrix}\mathbf{a_{3p_3}}\\ \mathbf{b_{3q_3}}\end{matrix}\,\middle|\, yt\right) dt = z^{-\alpha} G_{q_1,p_1:p_2,q_2:p_3,q_3}^{n_1,m_1:m_2,n_2:m_3,n_3}\left(\begin{matrix}1-\alpha-\mathbf{b_{1q_1}}\\ 1-\alpha-\mathbf{a_{1p_1}}\end{matrix}\,\middle|\, \begin{matrix}\mathbf{a_{2p_2}}\\ \mathbf{b_{2q_2}}\end{matrix}\,\middle|\, \begin{matrix}\mathbf{a_{3p_3}}\\ \mathbf{b_{3q_3}}\end{matrix}\,\middle|\, \frac{x}{z},\frac{y}{z}\right). \tag{9}$$

Hence, the solution for (9) is a Meijer G-function of two variables (also denoted [18] as extended generalized bivariate Meijer G-function (EGBMGF)), which is defined as (see II.13 in [21])

$$G_{p_1,q_1:p_2,q_2:p_3,q_3}^{m_1,n_1:m_2,n_2:m_3,n_3}\left(\begin{matrix}\mathbf{a_{1p_1}}\\ \mathbf{b_{1q_1}}\end{matrix}\,\middle|\, \begin{matrix}\mathbf{a_{2p_2}}\\ \mathbf{b_{2q_2}}\end{matrix}\,\middle|\, \begin{matrix}\mathbf{a_{3p_3}}\\ \mathbf{b_{3q_3}}\end{matrix}\,\middle|\, \frac{x}{z},\frac{y}{z}\right) = \frac{1}{(2\pi i)^2}\int_{L_2}\int_{L_1}\Psi_1(s+t)\,\Psi_2(s)\,\Psi_3(t)\, x^{-s} y^{-t} ds dt, \tag{10}$$

where

$$\Psi_k(\tau) = \frac{\prod_{j=1}^{m_k}\Gamma(b_{kj}+\tau)\prod_{j=1}^{n_k}\Gamma(1-a_{kj}-\tau)}{\prod_{j=n_k+1}^{p_k}\Gamma(a_{kj}+\tau)\prod_{j=m_k+1}^{q_k}\Gamma(1-b_{kj}-\tau)}, \quad k=1,2,3. \tag{11}$$

The contour L_1, in the s-plane, runs from $f_1 - i\infty$ to $f_1 + i\infty$ and separates the poles of $\Gamma(1-a_{1j}-s)$ $(j=1,\ldots,n_1)$, $\Gamma(1-a_{2j}-s)$ $(j=1,\ldots,n_2)$ from the poles of $\Gamma(b_{1j}+s)$ $(j=1,\ldots,m_1)$, $\Gamma(b_{2j}+s)$ $(j=1,\ldots,m_2)$, when $t \in L_2$. The contour L_2, in the t-plane, runs from $f_2 - i\infty$ to $f_2 + i\infty$ and separates the poles of $\Gamma(1-a_{1j}-s)$ $(j=1,\ldots,n_1)$, $\Gamma(1-a_{3j}-s)$ $(j=1,\ldots,n_3)$ from the poles of $\Gamma(b_{1j}+s)$ $(j=1,\ldots,m_1)$, $\Gamma(b_{3j}+s)$ $(j=1,\ldots,m_3)$, when $s \in L_1$.

According to the values of the parameters μ and m, the solutions for the ergodic capacity lead to different close-form expressions.

3.1. General Case: $(m-\mu) \notin \mathbb{Z}_0^+$. The parameters in the κ-μ shadowed model can take any arbitrary values; however $(m-\mu)$ cannot be a positive integer.

The Meijer G-identities corresponding to each of the special functions in (6) are [20]

$$\ln(1+x) = G_{2,2}^{1,2}\left(\begin{matrix}1,1\\ 1,0\end{matrix}\,\middle|\, x\right), \quad e^{-cx} = G_{0,1}^{1,0}\left(\begin{matrix}-\\ 0\end{matrix}\,\middle|\, cx\right), \quad {}_pF_q\left(\begin{matrix}a_p\\ b_q\end{matrix}\,\middle|\, x\right) = \frac{\Gamma(b_q)}{\Gamma(a_p)} G_{p,q+1}^{1,p}\left(\begin{matrix}1-a_p\\ 0,1-b_q\end{matrix}\,\middle|\, -x\right). \tag{12}$$

The double integral in (10) must satisfy the convergence theorems (see II.13 in [21]). In particular, the property ${}_1F_1(b-a,b;x) = e^x\, {}_1F_1(a,b;-x)$ must be applied to the confluent hypergeometric function so that the argument in the corresponding G-function is positive and the integral converges.

After some algebraic manipulations, the desired closed-form expression for the ergodic capacity is given by

$$C = \left(\frac{m}{\mu\kappa+m}\right)^{m-\mu} \frac{1}{\Gamma(\mu-m)\log(2)} \times G_{1,0:2,2:1,2}^{0,1:1,2:1,1}\left(\begin{matrix}1-\mu\\ -\end{matrix}\,\middle|\, \begin{matrix}1,1\\ 1,0\end{matrix}\,\middle|\, \begin{matrix}1+m-\mu\\ 0,1-\mu\end{matrix}\,\middle|\, \frac{\overline{\gamma}(\mu\kappa+m)}{m(1+\kappa)\mu}, \frac{\mu\kappa}{m}\right). \tag{13}$$

The above expression is valid for any set of parameters in the κ-μ shadowed model, except for particular relationships between μ and m that correspond to singularities of the gamma function. For these cases, $(m-\mu) \in \mathbb{Z}_0^+$, a different approach to determine the PDF of γ must be followed. This is done in the next section to obtain a new expression for the ergodic capacity.

3.2. Particular Case: $(m-\mu) \in \mathbb{Z}_0^+$. When $(m-\mu)$ is a positive integer, the singularities in (13) are solved by getting the PDF from the MGF of the κ-μ shadowed fading model. For this purpose, the inverse Laplace transform can be employed: $f_\gamma(\gamma) = \mathscr{L}^{-1}[\mathscr{M}_\gamma(-s); \gamma]$.

It is observed in (4) that the exponent of the s function in the numerator of $\mathscr{M}_\gamma(s)$ is a natural number, so the following expression (see 5.4(4) in [22]) can be used to calculate the inverse Laplace transform:

$$\begin{aligned}\mathscr{L}^{-1}\left[\Gamma(\nu+1)(s-\lambda)^n(s-\varepsilon)^{-\nu-1}\right] \\ = n!t^{\nu-n}e^{\varepsilon t}L_n^{\nu-n}(-(\varepsilon-\lambda)t),\end{aligned} \tag{14}$$

where L is the generalized Laguerre polynomial. Hence, the PDF is given by

$$\begin{aligned}f_\gamma(\gamma) = \frac{\mu^\mu m^m(1+\kappa)^\mu(m-\mu)!}{\Gamma(m)\overline{\gamma}(\mu\kappa+m)^m}\left(\frac{\gamma}{\overline{\gamma}}\right)^{\mu-1} \\ \times e^{-(\mu(1+\kappa)/\overline{\gamma})(m/(\mu\kappa+m))\gamma}L_{m-\mu}^{\mu-1}\left(\frac{\mu^2\kappa(1+\kappa)}{\mu\kappa+m}\frac{\gamma}{\overline{\gamma}}\right).\end{aligned} \tag{15}$$

Since $\mu - 1$ may be a real number and not a natural one, the expression for the generalized Laguerre polynomial must be written as (see 8.97 in [19]) $L_n^\alpha(x) = (\alpha+1)_n/n!\,{}_1F_1(-n, \alpha+1; x)$. Taking into account that ${}_1F_1(a,b;x) = \sum_{i=0}^{\infty}(a)_i/(b)_i x^i/i!$ and after some algebraic manipulations, the ergodic capacity yields

$$\begin{aligned}C = \left(\frac{m}{\mu\kappa+m}\right)^{m-\mu}\frac{(\mu)_{m-\mu}}{\Gamma(m)\log(2)} \\ \times\sum_{i=0}^{m-\mu}\left[\frac{(-(m-\mu))_i}{(\mu)_i i!}\left(-\frac{\mu\kappa}{m}\right)^i\right. \\ \left.\times G_{3,2}^{1,3}\left(\begin{matrix}1,1,1-(\mu+i)\\1,0\end{matrix}\middle|\frac{\overline{\gamma}(\mu\kappa+m)}{m(1+\kappa)\mu}\right)\right].\end{aligned} \tag{16}$$

For this particular case, the ergodic capacity depends on the sum of weighted Meijer G-functions, which is a simpler expression than the one presented for the general case. It can be proved that when m tends to infinity, (16) matches (6) in [5], which is the average channel capacity of the κ-μ model, after taking into account the following properties:

$$\begin{aligned}G_{p_0,q_0}^{m_0,n_0}\left(\frac{1}{z}\middle|\begin{matrix}a_1\cdots a_{p_0}\\b_1\cdots b_{q_0}\end{matrix}\right) = G_{q_0,p_0}^{n_0,m_0}\left(z\middle|\begin{matrix}1-b_1\cdots 1-b_{q_0}\\1-a_1\cdots 1-a_{p_0}\end{matrix}\right), \\ (a)_p = a(a+1)\cdots(a+p-1) = \frac{\Gamma(a+p)}{\Gamma(a)}.\end{aligned} \tag{17}$$

By setting $m = \mu$, the MGF expression boils down to

$$\mathscr{M}_\gamma(s) = \frac{(-m)^m}{\overline{\gamma}^m}\frac{1}{\left(s-\frac{m}{\overline{\gamma}}\right)^m}, \tag{18}$$

and the PDF is directly $f_\gamma(\gamma) = (m^m/(\overline{\gamma}^m\Gamma(m)))\gamma^{m-1}e^{-(m/\overline{\gamma})\gamma}$ and, by means of (5), the ergodic capacity is

$$C = \frac{1}{\log(2)\,\Gamma(m)}G_{3,2}^{1,3}\left(\begin{matrix}1,1,1-m\\1,0\end{matrix}\middle|\frac{\overline{\gamma}}{m}\right). \tag{19}$$

4. Numerical Results

This section presents numerical simulations to validate the proposed expressions of the ergodic capacity of a κ-μ shadowed fading channel.

For the particular cases $m = \mu$ and $(m-\mu) \in \mathbb{Z}^+$, the Meijer G-function can be evaluated by conventional mathematical packages. However, the Meijer G-function of two variables is not readily available. In the present work, the implementation presented in [18] is followed. The EGBMGF has been extended to any values of m_1 and n_1 in (10) and situations where the contours for the integrals cannot be a straight line parallel to the imaginary axis of the corresponding complex plane. See Appendix for a complete MATHEMATICA implementation of the function that has been used to obtain the numerical results for the ergodic capacity in the general case.

To check the analytical expressions, numerical simulations have been carried out by generating random numbers according to the physical model and the corresponding classical distributions. However, the physical model cannot be used directly when μ is not a natural number. In that situation, a sampled version of the CDF in (3) has been calculated for the selected set of physical parameter values. Afterwards, random numbers have been generated with a uniform distribution and then mapped into a κ-μ shadowed distribution by using the inverse CDF method.

In Figure 1, the ergodic capacity for three different sets of parameters of the fading model is drawn. The parameters have been selected to showcase the three types of expressions obtained for the ergodic capacity (13), (16), and (19). In all cases the simulations and the corresponding analytical results show perfect agreement.

Figures 2–4 highlight the influence of the parameters on the channel capacity, according to the physical model. As mentioned before, the m-parameter represents the level of fluctuation due to shadowing in the dominant component and the κ-parameter indicates the ratio between the dominant components and the scattered waves (and models the fading channel). For large κ values, more power is present in the dominant component with respect to the scattered waves, while, for large m, the power of the dominant component is more stable and therefore there is less shadowing. In Figures 2–4, the sensitivity of the ergodic capacity on the m-parameter is shown at different values of κ (hence different dominant components importance). For the remainder of the paper, the parameter μ has been set to 3, which corresponds to a situation where the scattered waves arrive in the receiver organized in three clusters.

In Figure 2, there is a strong dominant component ($\kappa = 5$) and the influence of m on the ergodic capacity is very significant. This dependency on m increases with γ (the average received signal to noise ratio). For signal to noise ratios above

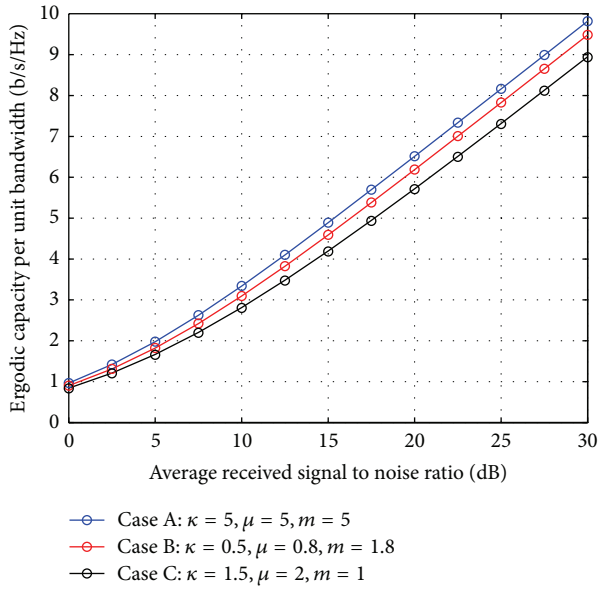

FIGURE 1: Representation of mean capacity values for different kinds of analytical solutions. The marks correspond to results obtained by numerical simulation.

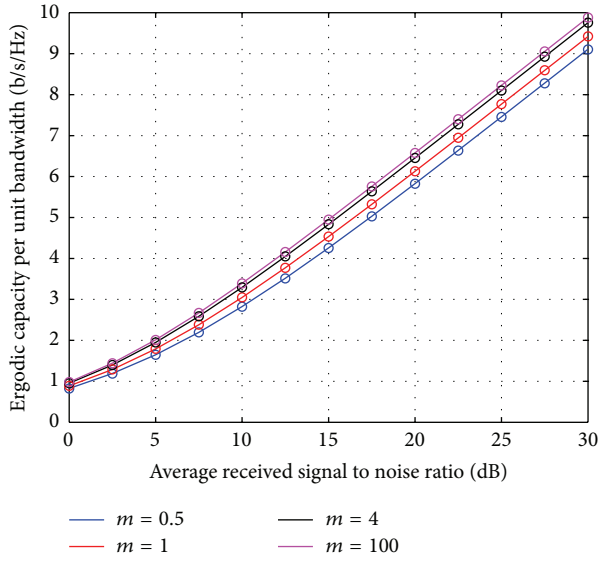

FIGURE 2: Influence of shadowing m-parameter on the mean capacity values when the dominant component is more powerful than the scattered waves ($\kappa = 5$). The value of μ-parameter is set to 3 in all curves. The marks correspond to results obtained by numerical simulation.

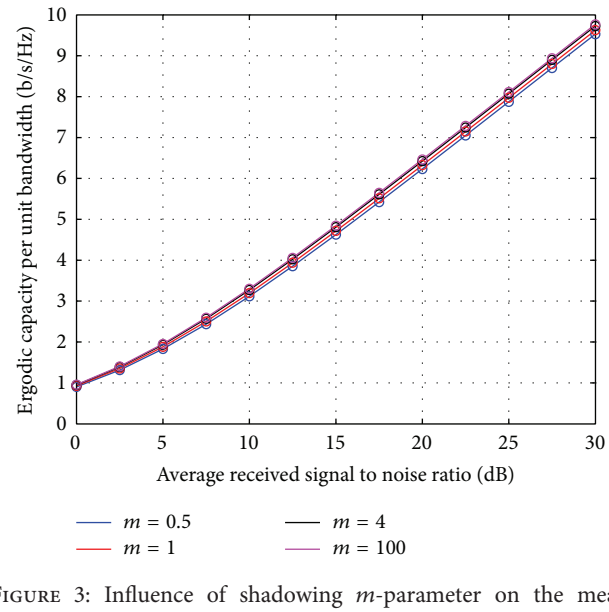

FIGURE 3: Influence of shadowing m-parameter on the mean capacity values when the dominant component has the same power as the scattered waves ($\kappa = 1$). The value of μ-parameter is set to 3 in all curves. The marks correspond to results obtained by numerical simulation.

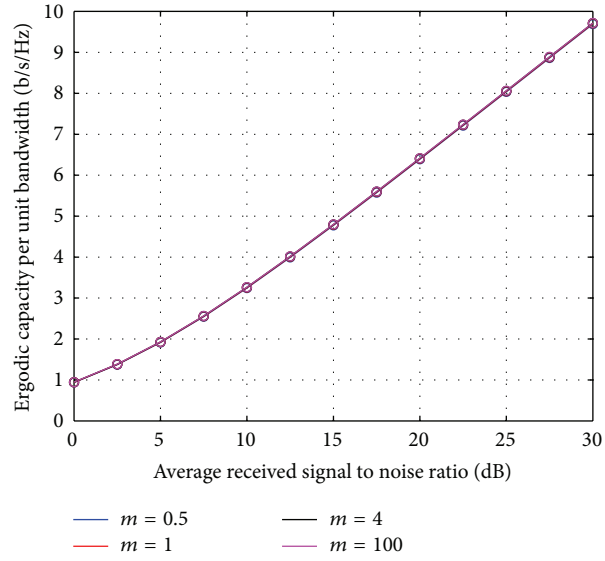

FIGURE 4: Influence of shadowing m-parameter on the mean capacity values when the dominant component is less powerful than the scattered waves ($\kappa = 0.2$). The value of μ-parameter is set to 3 in all curves. The marks correspond to results obtained by numerical simulation.

15–20 dB, the ergodic capacity exhibits a quasilinear behavior, with a constant difference between the minimum capacity (at $m = 0.5$) and maximum (at $m = 100$) of approximately 0.8 bit/s/Hz.

In Figure 3, the power of the dominant component is the same as the scattered waves ($\kappa = 1$) and hence m has a lower influence and there is less than 0.25 bit/s/Hz difference between the capacities at lowest and highest value of m.

Finally, in Figure 4, the dominant component is very weak compared to the scattered components ($\kappa = 0.2$) and the impact of m on the ergodic capacity is negligible.

Table 1 summarizes the ergodic capacity and its dependency on both κ and m parameters. It can be seen that, under a weak shadowing condition (large m), the ergodic capacity increases with κ, while, under a strong shadowing

```
Clear All;
S[{a1st_, b1st_}, {a2s_, b2s_}, {a3t_, b3t_}, μS_, mS_, {zs_, zt_}]:= Module[{},
(*Function Φ1(s + t)*)
Past = Function[u, Product[Gamma[1 − a1st[[1, n]] − u], {n, 1, Length[a1st[[1]]]}]];
Qast = Function[u, Product[Gamma[a1st[[2, n]] + u], {n, 1, Length[a1st[[2]]]}]];
Pbst = Function[u, Product[Gamma[b1st[[1, n]] + u], {n, 1, Length[b1st[[1]]]}]];
Qbst = Function[u, Product[Gamma[1 − b1st[[2, n]] − u], {n, 1, Length[b1st[[2]]]}]];
Mst = Function[u, Past[u] ∗ Pbst[u]/(Qast[u] Qbst[u])];
(*Function Φ2(s)*)
Pas = Function[u, Product[Gamma[1 − a2s[[1, n]] − u], {n, 1, Length[a2s[[1]]]}]];
Qas = Function[u, Product[Gamma[a2s[[2, n]] + u], {n, 1, Length[a2s[[2]]]}]];
Pbs = Function[u, Product[Gamma[b2s[[1, n]] + u], {n, 1, Length[b2s[[1]]]}]];
Qbs = Function[u, Product[Gamma[1 − b2s[[2, n]] − u], {n, 1, Length[b2s[[2]]]}]];
Ms = Function[u, Pas[u] ∗ Pbs[u]/(Qas[u] Qbs[u])];
(*Function Φ3(t)*)
Pat = Function[u, Product[Gamma[1 − a3t[[1, n]] − u], {n, 1, Length[a3t[[1]]]}]];
Qat = Function[u, Product[Gamma[a3t[[2, n]] + u], {n, 1, Length[a3t[[2]]]}]];
Pbt = Function[u, Product[Gamma[b3t[[1, n]] + u], {n, 1, Length[b3t[[1]]]}]];
Qbt = Function[u, Product[Gamma[1 − b3t[[2, n]] − u], {n, 1, Length[b3t[[2]]]}]];
Mt = Function[u, Pat[u] ∗ Pbt[u]/(Qat[u] Qbt[u])];
MT = Function[u, v, Mst[u + v] ∗ Ms[u] ∗ Mt[v]];
(*Countour limiters*)
Zs = zs; (*x*)
Zt = zt; (*y*)
W = 50;
Wp = 10; (*When it is necessary to apply integration by parts. Only for t variable*)
Rs = −1/4;
If[(μS − mS) > 0,
   Rt = (μS − mS)/2;
   (*Final Evaluation*)
   Print["Numerical Integration:"];
   value = 1/(2πI)^2 NIntegrate[MT[s, t] Zs^−s Zt^−t, {s, Rs − I ∗ W, Rs + I ∗ W}, {t, Rt − I ∗ W, Rt + I ∗ W}],
   PosPoleT = Ceiling[Abs[μS − mS]] + (μS − mS);
   NegPoleT = Floor[Abs[μS − mS]] + (μS − mS);
   Rt1 = PosPoleT/2;
   Rt2 = NegPoleT/2;
    (*Final Evaluation*)
   Print["Numerical Integration by parts:"];
   valIni = 1/(2πI)^2 NIntegrate[MT[s, t] Zs^−s Zt^−t, {s, Rs − I ∗ W, Rs + I ∗ W}, {t, Rt1 − I ∗ W, Rt1 − I ∗ Wp}];
   nIter = Abs[Floor[μS − mS]];
   val1T = Sum[1/(2πI)^2 NIntegrate[MT[s, t] Zs^−s Zt^−t, {s, Rs − I ∗ W, Rs + I ∗ W}, {t, (Rt1 − n + 1) − I ∗ Wp,
         (Rt1 − n + 1) + I ∗ Wp}], {n, 1, nIter}];
   val2T = Sum[1/(2πI)^2 NIntegrate[MT[s, t] Zs^−s Zt^−t, {s, Rs − I ∗ W, Rs + I ∗ W}, {t, (Rt1 − n + 1) + I ∗ Wp,
         (Rt2 − n + 1) + I ∗ Wp}], {n, 1, nIter}];
   val3T = Sum[1/(2πI)^2 NIntegrate[MT[s, t] Zs^−s Zt^−t, {s, Rs − I ∗ W, Rs + I ∗ W}, {t, (Rt2 − n + 1) + I ∗ Wp,
         (Rt2 − n + 1) − I ∗ Wp}], {n, 1, nIter}];
   val4T = Sum[1/(2πI)^2 NIntegrate[MT[s, t] Zs^−s Zt^−t, {s, Rs − I ∗ W, Rs + I ∗ W}, {t, (Rt2 − n + 1) − I ∗ Wp,
         (Rt1 − n) − I ∗ Wp}], {n, 1, nIter}];
   valFin = 1/(2πI)^2 NIntegrate[MT[s, t] Zs^−s Zt^−t, {s, Rs − I ∗ W, Rs + I ∗ W}, {t, (Rt1 − nIter) − I ∗ Wp,
         (Rt1 − nIter) + I ∗ W}];
   value = valIni + valFin + val1T + val2T + val3T + val4T];
   (*Returning back the value*)
   Return[value];
];
(*End of MEGBMGF*)
```

Algorithm 1: Implementation of the bivariate Meijer G-function in Mathematica software (*modification of the EGBMGF [18] to conform the κ-μshadowed model*).

Table 1: Ergodic capacity (in bit/s/Hz) for extreme values of m (μ = 3 and $\overline{\gamma}$ = 30 dB).

	$m = 0.5$	$m = 100$
$\kappa = 5$	9.109	9.885
$\kappa = 1$	9.530	9.770
$\kappa = 0.2$	9.692	9.720

condition (low m), the ergodic capacity decreases with κ as the contribution of the scattered waves is advantageous.

5. Conclusion

In the paper, an exact closed-form expression is presented for the ergodic capacity of communications channels that exhibit a fading according to the κ-μ shadowed distribution. These communication channels can be found in systems where a line-of-sight component experiences shadowing, for example, in land mobile satellite systems, underwater acoustic communications, or body centric communications. The derived analytical expressions have been validated against numerical simulations for different capacity curves. The influence of parameters on the shadowing level has been also investigated. The results contained in this work can be used for future evaluation of channels communication performance on different applications.

Appendix

See Algorithm 1.

Conflict of Interests

The authors declare that there is no conflict of interests regarding the publication of this paper.

Acknowledgments

This work has been supported by FEDER and the Spanish and Andalusian Governments, under Projects TEC2011-25473 and P11-TIC-8238, respectively.

References

[1] T. S. Rappaport, *Wireless Communications. Principles and Practice*, Prentice Hall, Englewood Cliffs, NJ, USA, 1996.

[2] W. R. Braun and U. Dersch, "A physical mobile radio channel model," *IEEE Transactions on Vehicular Technology*, vol. 40, no. 2, pp. 472–482, 1991.

[3] A. Goldsmith, *Wireless Communications*, Cambridge University Press, 2005.

[4] M. D. Yacoub, "The $\kappa - \mu$ and the $\eta - \mu$ distribution," *IEEE Antennas and Propagation Magazine*, vol. 49, pp. 68–81, 2007.

[5] D. B. da Costa and M. D. Yacoub, "Average channel capacity for generalized fading scenarios," *IEEE Communications Letters*, vol. 11, no. 12, pp. 949–951, 2007.

[6] X. Wang and N. C. Beaulieu, "Switching rates of two-branch selection diversity in $\kappa - \mu$ and $\alpha - \mu$ distributed fadings," *IEEE Transactions on Wireless Communications*, vol. 8, no. 4, pp. 1667–1671, 2009.

[7] R. Cogliatti, R. A. A. de Souza, and M. D. Yacoub, "Practical, highly efficient algorithm for generating $\kappa - -\mu$ and $\eta - -\mu$ variates and a near-100% efficient algorithm for generating $\alpha - -\mu$ variates," *IEEE Communications Letters*, vol. 16, no. 11, pp. 1768–1771, 2012.

[8] K. P. Peppas, "Sum of nonidentical squared $\kappa - \mu$ Variates and applications in the performance analysis of diversity receivers," *IEEE Transactions on Vehicular Technology*, vol. 61, no. 1, pp. 413–419, 2012.

[9] P. Sofotasios, E. Rebeiz, L. Zhang et al., "Energy detection based spectrum sensing over $\kappa - \mu$ and $\kappa - \mu$ extreme fading channels," *IEEE Transactions on Vehicular Technology*, vol. 62, no. 3, pp. 1031–1040, 2013.

[10] S. L. Cotton, "A statistical model for shadowed body-centric communications channels: theory and validation," *IEEE Transactions on Antennas and Propagation*, vol. 62, no. 3, pp. 1416–1424, 2014.

[11] I. Trigui, A. Laourine, S. Affes, and A. Stéphenne, "Performance analysis of mobile radio systems over composite fading/shadowing channels with co-located interference," *IEEE Transactions on Wireless Communications*, vol. 8, no. 7, pp. 3448–3453, 2009.

[12] J. Zhang, M. Matthaiou, Z. Tan, and H. Wang, "Performance analysis of digital communication systems over composite $\eta - -\mu$/gamma fading channels," *IEEE Transactions on Vehicular Technology*, vol. 61, no. 7, pp. 3114–3124, 2012.

[13] S. R. Panic, D. M. Stefanović, I. M. Petrović, M. Č. Stefanović, J. A. Anastasov, and D. S. Krstić, "Second-order statistics of selection macro-diversity system operating over Gamma shadowed $\kappa - -\mu$ fading channels," *EURASIP Journal on Wireless Communications and Networking*, vol. 2011, article 151, 2011.

[14] P. C. Sofotasios and S. Freear, "On the κ-μ/gamma composite distribution: a generalized multipath/shadowing fading model," in *Proceedings of the IEEE International Microwave and Optoelectronics Conference (IMOC' 11)*, Natal, Brazil, October 2011.

[15] A. Abdi, W. C. Lau, M. Alouini, and M. Kaveh, "A new simple model for land mobile satellite channels: First-and second-order statistics," *IEEE Transactions on Wireless Communications*, vol. 2, no. 3, pp. 519–528, 2003.

[16] F. Ruiz-Vega, M. C. Clemente, J. F. Paris, and P. Otero, "Rician shadowed statistical characterization of shallow water acoustic channels for wireless communications," in *Proceedings of the Underwater Communications Conference*, Sestri, Italy, September 2012.

[17] J. F. Paris, "Statistical characterization of $\kappa - -\mu$ shadowed fading channels," *IEEE Transactions on Vehicular Technology*, vol. 63, no. 2, pp. 518–526, 2014.

[18] I. S. Ansari, S. Al-Ahmadi, F. Yilmaz, M. S. Alouini, and H. Yanikomeroglu, "A new formula for the BER of binary modulations with dual-branch selection over generalized-composite fading channels," *IEEE Trans. on Communications*, vol. 59, no. 10, pp. 2654–2658, 2011.

[19] I. S. Gradshteyn and I. M. Ryzhik, *Table of Integrals, Series, and Products*, Academic Press, 7th edition, 2007.

[20] Wolfram Research, MeijerG, http://functions.wolfram.com/HypergeometricFunctions/MeijerG/.

[21] T. H. Nguyen and S. B. Yakubovich, *The Double Mellin-Barnes Type Integrals and Their Applications to Convolution Theory*, World Scientific, 1992.

[22] A. Erdelyi, *Tables of Integral Transforms I*, McGraw Hill, New York, NY, USA, 1954.